Ryszard Krawczyk, Jacek Słania

Analysis of Surface Quality after Oxygen Cutting

Abstract: The article discusses tests concerning surface quality after the oxygen cutting of steel plates of various thicknesses. The study involved visual tests, macro and microscopic metallographic tests as well as hardness measurements and the identification of hardness distribution in the cut zone and in the heat affected zone.

Keywords: oxygen cutting, cutting technique, cutting equipment, surface quality

DOI: *10.17729/ebis.2022.2/4*

Introduction

In oxygen cutting the heat used in the process results from the burning of a gas mixture enriched with oxygen, being the catalyst of a further exothermic reaction aimed to separate elements subjected to cutting. To oxidise metal being cut, an area subjected to cutting is affected by the stream of oxygen surrounded by a heating flame. The oxygen cutting process involves the division of solid-state metal heated up to an ignition point. During the process, the metal is locally oxidised (burnt), whereas the liquid products of the oxidation reaction are blown out of the cutting gap (partly by the heat source consisting of the gaseous flame and the oxygen stream characterised by high purity and high kinetic energy) [1–8]. There are several types of flames, with cutting being performed using the oxydising flame. The applications of individual types of flames are the following:

- oxydising flame is used primarily to separate metals; the inflammable gas-oxygen ratio is higher than 1.3:1,
- normal flame, used primarily in welding processes (also often used to heat up elements); the inflammable gas-oxygen ratio is restricted within the range of 1:1 to maximally 1.3:1,
- carburising flame is used for the welding of aluminium and its alloys; the flame is formed in excess inflammable gas [1, 2].

The primary disadvantage of the above-named heat source is its dissipation, where not only the cut zone but also the area adjacent to it are heated, which in turn, leads to the degradation of the material.

The process technology is very important; the process parameters should be adjusted so that the most favourable shape of the surface could be maintained without compromising the proper direction of flame movement and a relatively high cutting rate [1, 9–11].

Tests

Specimens used in the tests were made of 20 mm, 12 mm and 6 mm thick steel S355J2 and cut out of the plates using an EasyTherm Messer machine. The method of cutting was the same

Dr hab. inż. Ryszard Krawczyk, Professor at the Częstochowa University of Technology;
prof. dr hab. inż. Jacek Słania – Częstochowa University of Technology; Faculty of Mechanical Engineering and Computer Science / Łukasiewicz Research Network - Instytut Spawalnictwa

in relation to each plate thickness. To maintain the rectangular shape of the specimen without cutting-triggered damage (Fig. 1), the punch-through was performed outside the specimen area (Figure 1).

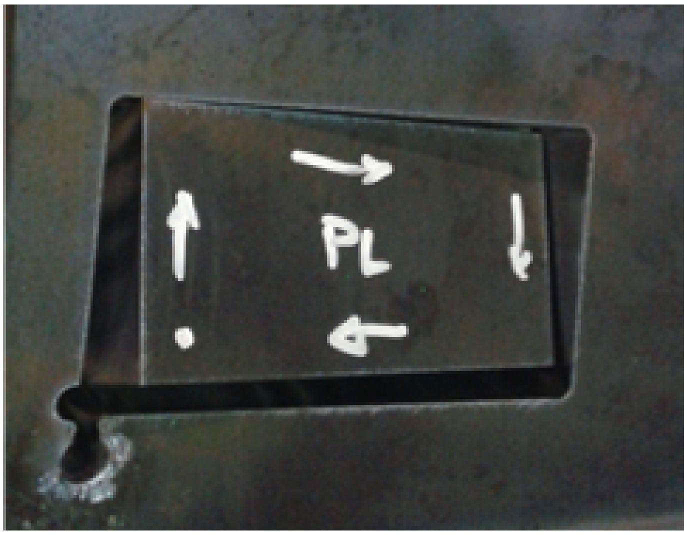

Fig. 1. Method applied to cut the specimens out of the test plates

The above-presented sampling method and the assumed shape additionally enabled the identification of certain shortcomings of the process. Surfaces subjected to cutting were deliberately placed so that it would be possible to analyse parallelism or perpendicularity as well as to identify the process-related defects following the change of the cutting direction. The visual inspection and assessment (after cutting) were followed by the further sampling of specimens (30 mm × 50 mm) across the longer edge. The oxygen cutting process parameters are presented in Table 1.

Table 1. Parameters adjusted during the oxygen cutting of the test materials (performed using the EasyTherm Messer machine)

Plate thickness, mm	6	12	20
Cutting rate, mm/min	635	550	460
Cutting gas pressure, bar	3.0	6.5	6.6
Heating pressure, bar	1.5	1.5	1.0
Heating time, s	7	7.5	8
Cutting gap width, mm	1.5	2.2	2.2
Distance between the torch and the plate, mm	5	6	6

The visual tests involved the cut surface and consisted in the detailed assessment of the profile of the surface, its general condition as well as the degree of its degradation. Further analysis involved the sampling of metallographic specimens, including the entire cross-section of the specimen and the cut edge. The surface of the metallographic specimens was subjected to etching (aimed to obtain material for further macro and microscopic tests as well as hardness measurements, involving the cut surface and the heat affected zone). The etchant used in the tests was Nital (8% and 5%). The specimens prepared in the above-presented manner were subjected to tests discussed in the remainder of the article.

Macroscopic tests involved the visual assessment of the surface, the edge of the cut-out and the width of the HAZ. The tests were performed in three stages, i.e. without image magnification (i.e. observations by the unaided eye) and with magnified images (to obtain better representation of results). **Microscopic tests** involved the entire cross-section with particular attention paid to the heat affected zone (HAZ) and the cut edge. The tests were performed using a digital microscope (Olympus) and a magnification of x50. **Hardness measurements** were performed on the surface of the cross-section, i.e. from its axis in the direction of the cut edge and in the HAZ. The measurements involved the use of the Vickers hardness tests (HV5) and an HPO 250 hardness tester.

Test results

Visual tests of the cut surface

The first stage involved the visual assessment of all the specimens directly after cutting (without being subjected to any form of treatment). The assessment was performed in relation to conditions of the stabilised oxygen cutting process. The specimens (of various thicknesses) are presented in Figures 2 through 4. Figure 2 presents (from various sides) the surface of the specimen cut out of the 20 mm thick plate.

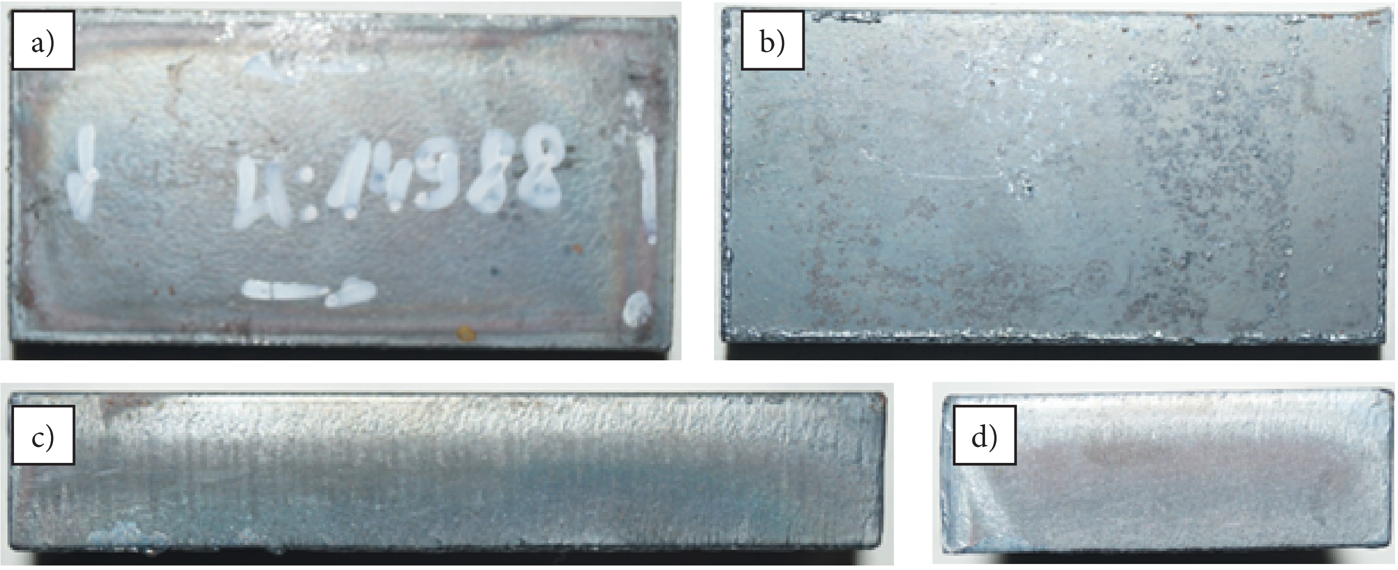

Fig. 2. Surface of the 20 mm thick plate after oxygen cutting: a) upper, b) lower c) longer side and d) shorter side

After oxy-acetylene cutting, the surface of the 20 mm thick plates could be regarded as smooth. The area where the cutting of the plate was initiated contained a clearly visible mark triggered by the penetration of the plate. It was also possible to notice the tendency of plate contour profile rounding where the direction of burning changed. The cut edge was perpendicular to the surface of the material subjected to cutting; no significant bevelling of the plate was observed. The lower part of the plate contained visible traces of cinder and overhangs (on the lower edge of the plate). The cut edge in the upper part contained visible grooves. The performance of the welding process required the removal of the aforementioned cinder. Figure 3 presents (from various sides) the surface of the specimen cut out of the 12 mm thick plate.

The surface of the 12 mm thick plates subjected to oxy-acetylene cutting could be regarded as smooth with slightly visible grooves. The area where the cutting of the plate was initiated contained a clearly visible mark triggered by the penetration of the plate. It was also possible to notice the tendency of plate contour profile rounding where the direction of cutting changed as well as the partial melting of the upper edge of the plate and the burning out of grooves. The lower part of the plate edge contained traces of cinder and overhangs. By contrast with the thicker plates, the edge showed the tendency of perpendicularity deviations. The foregoing could imply the use of improper materials. In addition, (as regards the 12 mm thick plate) the side surface was covered with hard-to-remove oxides, requiring the

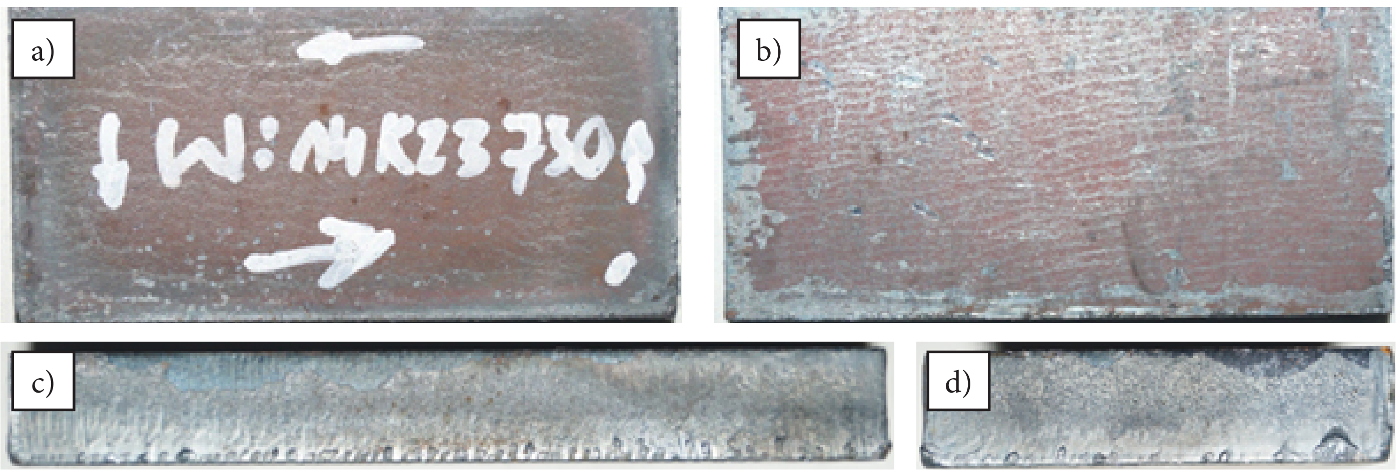

Fig. 3. Surface of the 12 mm thick plate after oxygen cutting: a) upper, b) lower c) longer side and d) shorter side

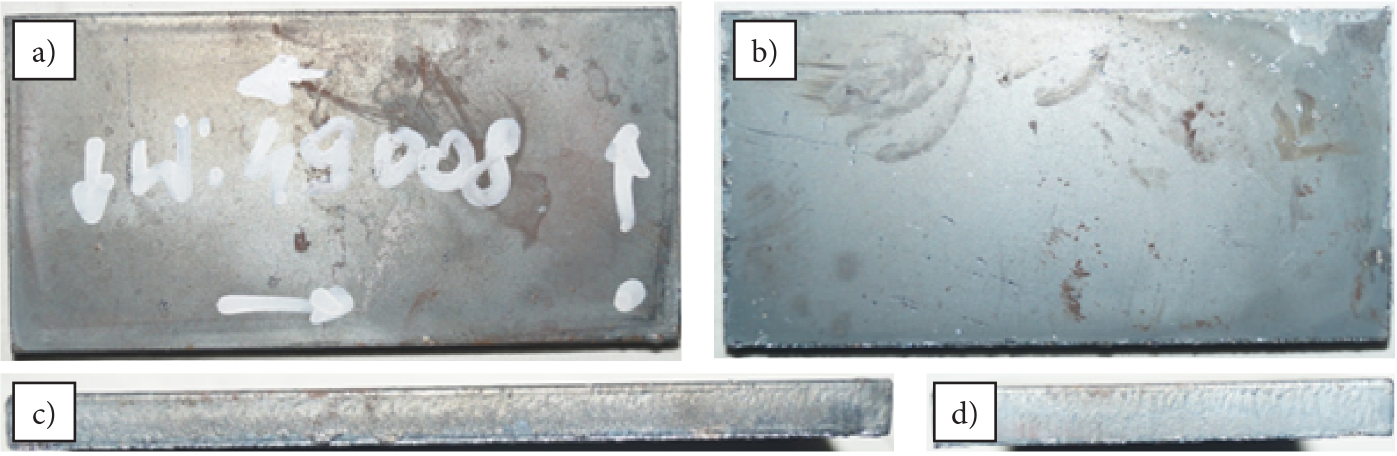

Fig. 4. Surface of the 6 mm thick plate after oxygen cutting: a) upper, b) lower c) longer side and d) shorter side

application of additional processing (aimed to safely perform further processes). Figure 4 presents (from various sides) the surface of the specimen cut out of the 6 mm thick plate.

The most favourable surface parameters (after oxygen cutting) were those of the specimens cut out of the 6 mm thick plate. The surface also contained the visible area of penetration, yet it was so small that it could be regarded as negligible. The edge of the plate was also characterised by the presence of grooves in the upper plane, yet not as clearly visible as those observed in relation to the thicker plates. The lower surface of the plate contained slight traces of cinder and a small amount of overhangs. On the basis of the above-presented observations it could be stated that an increase in the thickness of a given element subjected to cutting was accompanied by deteriorating surface quality, which, in turn, could imply the improper adjustment of process parameters. However, it should be noted that the cut-out specimens only represented fragments of the plates and, as a result, certain features characteristic of a given process might have remained unnoticed. Oxygen-based processes are characterised by the significant concentration of energy affecting a relatively small area, which could lead to shape deformations when cutting thin plates/sheets and, consequently, adversely affect the shape of a predefined cut-out.

To analyse the cross-section in more detail, each edge (after cutting) was observed at magnification (Figures 5–7). Figure 5 presents the cross-section of the edge of the specimen (designated with the rectangular rim) cut out of the 20 mm thick plate.

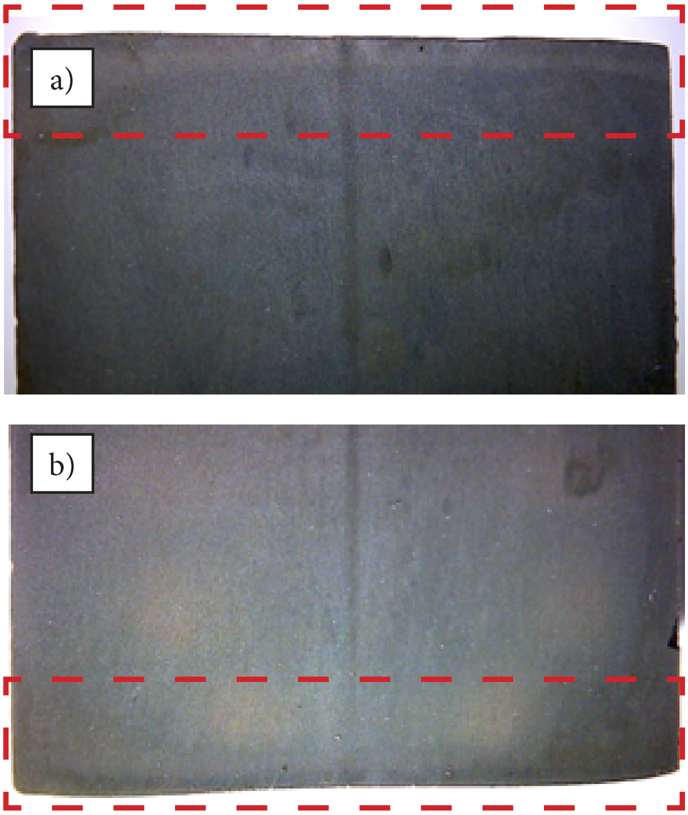

Fig. 5. Edge of the 20 mm thick plate after oxygen cutting from side a) A and b) B

Figures 5a and 5b present the edges of the plate after cutting (side A and B). In relation to the 20 mm thick sheets, the cross-sectional reduction was significant. It was also possible to notice the clearly visible lack of edge rectilinearity. The deformation of the edge was greater in the upper surface of the plate (exposed to an intense exothermic reaction leading to the

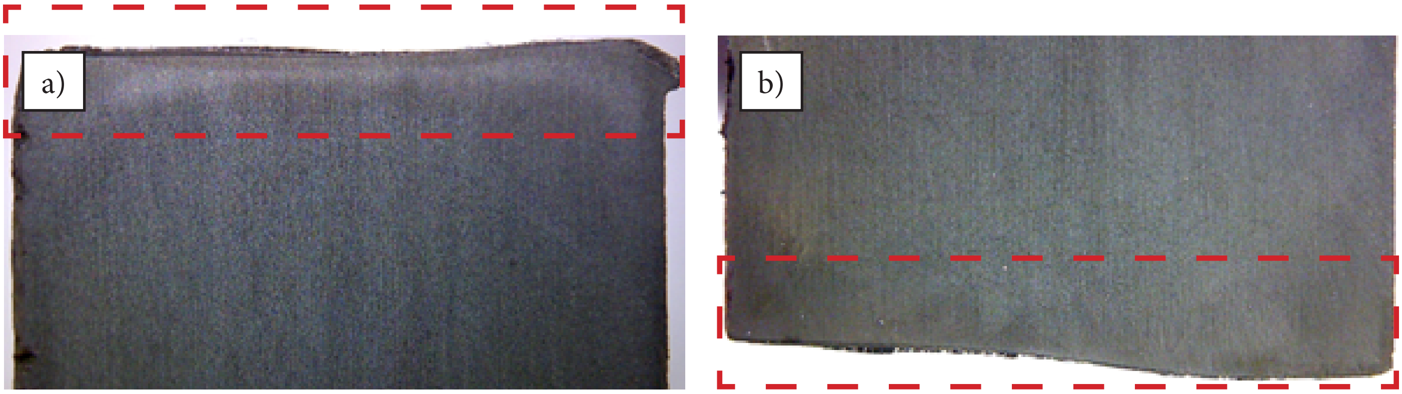

Fig. 6. Edge of the 12 mm thick plate after oxygen cutting from side a) A and b) B

oxidation of the material at a certain depth). In the metallographic specimen it was also possible to observe the heat affected zone (of a significant size in relation to the process (Table 2)). Figure 6 presents the cross-section of the edge of the specimen (designated with the rectangular rim) cut out of the 12 mm thick plate.

The metallographic specimens (Figures 6a and 6b) made of the 12 mm thick specimens subjected to oxygen cutting revealed the entirely different nature of the edges. One of the edges was characterised by the significant depletion of the cross-section, whereas the other edge did not reveal such a tendency. The above-named phenomenon could be ascribed to the "upsetting" of process conditions. The metallographic specimens also revealed the width of the heat affected zone, which also proved significant in relation to the specimen having a thickness of 12 mm. Near the lower surface of the plate it was possible to notice a significant overhang and traces of cinder.

Figure 7 presents the cross-section of the edge of the specimen (designated with the rectangular rim) cut out of the 6 mm thick plate.

In terms of the specimen having a thickness of 6 mm, the oxygen cutting process was responsible for the highest heat input (Figures 7a and7b). In comparison with the thickness of the material, the heat affected zone was very wide. The loss of material was also significant as regards the edge designated as B. The upper part of the edge contained visible partial burning. The macroscopic metallographic specimen revealed the presence of an overhang on one of the edges. The above-presented appearance and the nature of the edge after oxygen cutting confirmed that the process significantly degraded the edge of the material subjected to cutting and that the application of oxygen cutting was unfavourable in relation to thin elements.

The width of the heat affected zone significantly affected the element subjected to cutting. The HAZ reflected the degree of material degradation triggered by the heat source applied in the process. The heat affected zone was the area of many structural transformations, changes of mechanical properties and a local increase in hardness. The measurement results concerning the HAZ width, obtained in the macroscopic tests, are presented in Figure 8 and Table 2.

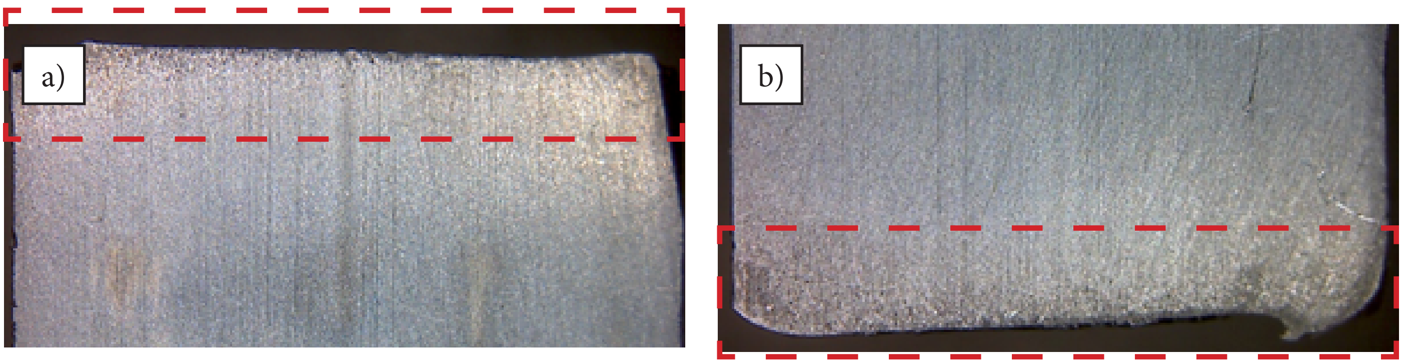

Fig. 7. Edge of the 6 mm thick plate after oxygen cutting from side a) A and b) B

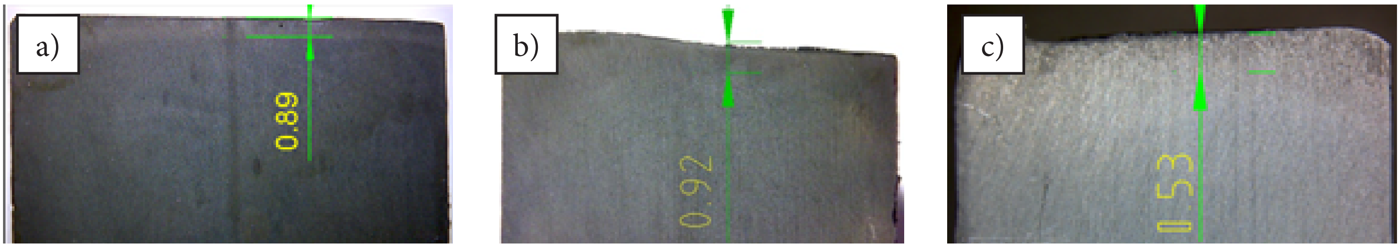

Fig. 8. Width of the HAZ after the oxygen cutting of the plates having a thickness of a) 20 mm, b) 12 mm and c) 6 mm

Table 2. Width of the HAZ after the oxygen cutting of the plates having a thickness of 20 mm, 12 mm and 6 mm

Plate thickness, mm	20	12	6
HAZ width, mm	0.89	0.92	0.53

Microscopic tests

The detailed analysis of the cut edge of each specimen involved the performance of microscopic tests, aimed to identify the shape of the edge and precisely determine the width of the HAZ in three areas, i.e. in the upper surface, in the central part of the cross-section and in the lower area of the plate. In relation to all thicknesses, the tests were performed using a magnification of x50. Only one reference edge of the cross-section was subjected to the test. Figures 9–11 present the microscopic images of the metallographic specimens of the plates having a thickness of 20 mm, 12 mm and 6 mm respectively (from the upper through the central to the lower zone):

The values of the HAZ identified in the microscopic tests in relation to the three zones of the plates having a thickness of 20 mm, 12 mm and 6 mm are presented in Table 3.

Hardness measurements in the cutting zone

Thermal cutting not only triggers structural transformations but is also responsible for a local increase in hardness, which, in turn, adversely affects the mechanical workability or weldability of materials. The hardness measurements involved the plate specimens used in the previous tests. The first measurements were

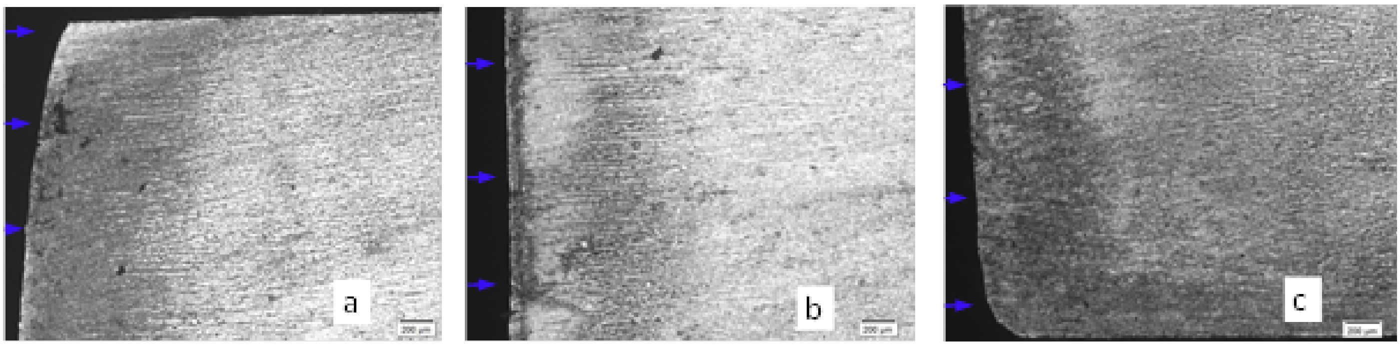

Fig. 9. Microscopic metallographic specimens of the 20 mm thick plate after oxygen cutting: a) upper zone near the heat source, b) central zone and c) lower zone

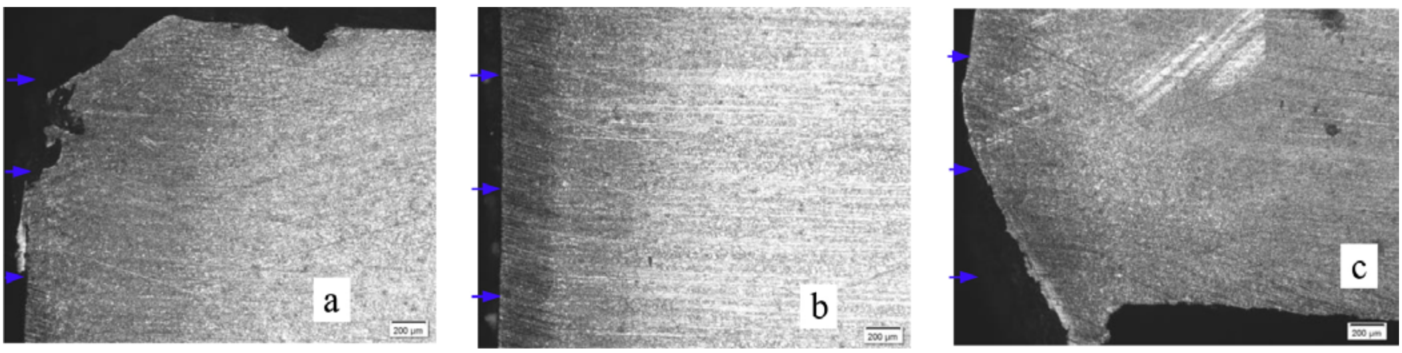

Fig. 10. Microscopic metallographic specimens of the 12 mm thick plate after oxygen cutting: a) upper zone near the heat source, b) central zone and c) lower zone

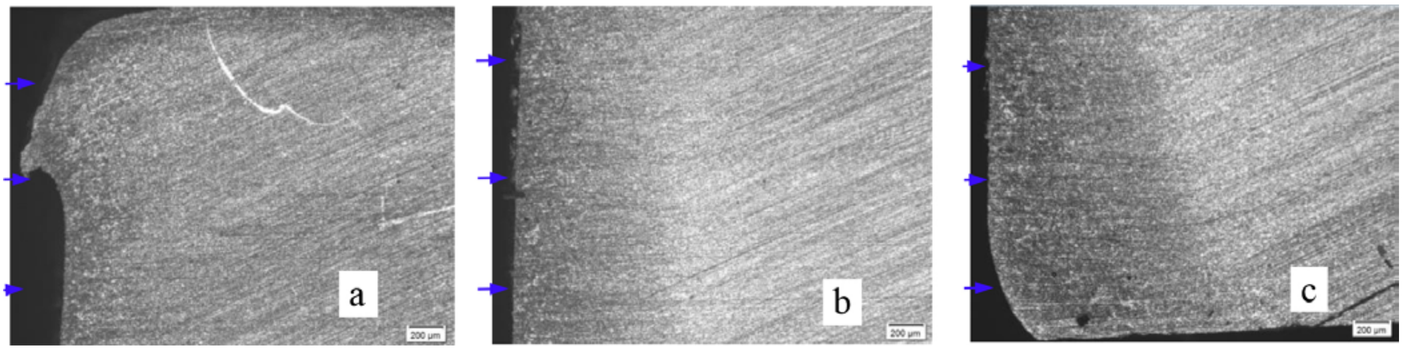

Fig. 11. Microscopic metallographic specimens of the 6 mm thick plate after oxygen cutting: a) upper zone near the heat source, b) central zone and c) lower zone

Table 3. Width of the HAZ in relation to the 20 mm, 12 mm and 6 mm thick plates

HAZ width measurement zone	**HAZ width in relation plate thickness**		
	20 mm	12 mm	6 mm
upper	1380 μm	1000 μm	1220 μm
central	1000 μm	880 μm	900 μm
lower	910 μm	900 μm	810 μm

Table 4. Hardness measurement results after the oxygen cutting of 20 mm, 12 mm and 6 mm thick plates

Plate thickness, mm	Hardness HV5 / Distance from the cut edge, mm											Average hardness on the cut surface, HV5
20	566	501	332	289	244	232	214	210	208	204	201	271
	0.19	0.23	0.39	0.4	0.6	0.62	0.7	0.7	0.9	0.92	1.0	
12	299	296	286	262	216	216	214	208	204			252
	0.22	0.24	0.25	0.3	0.5	0.55	0.52	0.6	0.7			
6	210	210	204	195	185							237
	0.25	0.3	0.5	0.7	0.9							

performed on the cross-section, perpendicularly to the cut edge - in various areas (near the edge and in the stabilized zone, i.e. where hardness no longer changed). The subsequent tests involved the cut surface. Afterwards, the results of all measurements were compared and used to identify hardness distribution. The results of hardness measurements are presented in Table 4, whereas hardness distribution is presented in Figures 12–14.

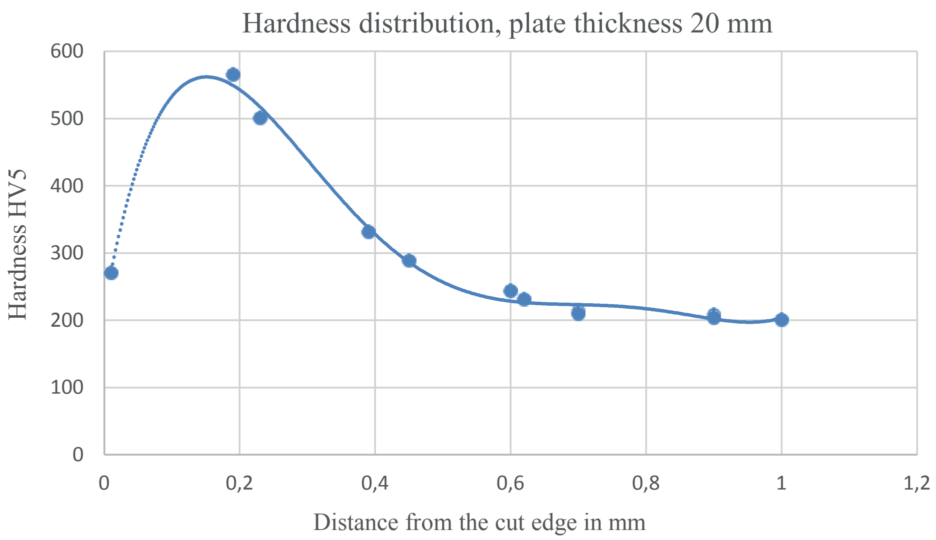

Fig. 12. Hardness distribution in the cross-section of the 20 mm thick specimen subjected to oxygen cutting

In oxygen-based processes, the temperature of the flame significantly longer affects a given workpiece (even after its division), leading to a decrease in the cooling rate. It is also possible to observe the fluidisation of the material on its edge, which, in terms of oxygen cutting, significantly reduces hardness.

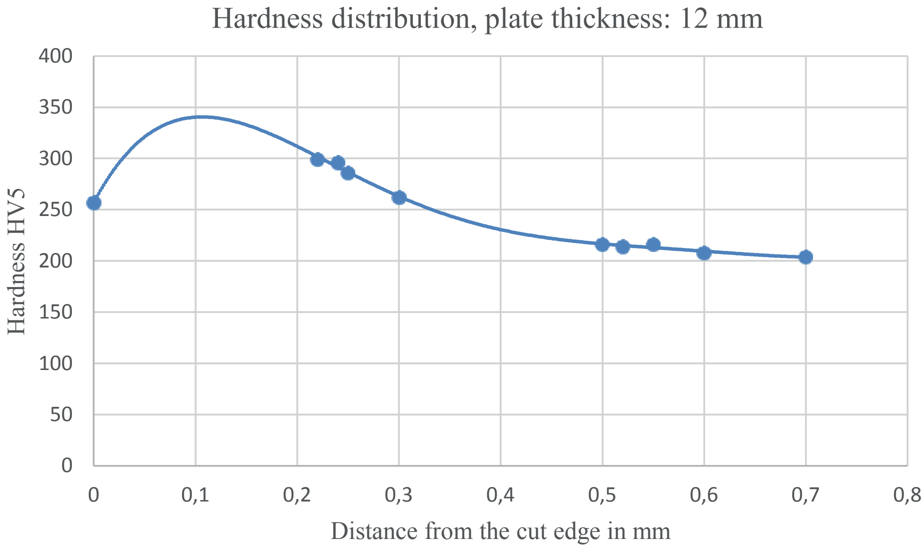

Fig. 13. Hardness distribution in the cross-section of the 12 mm thick specimen subjected to oxygen cutting

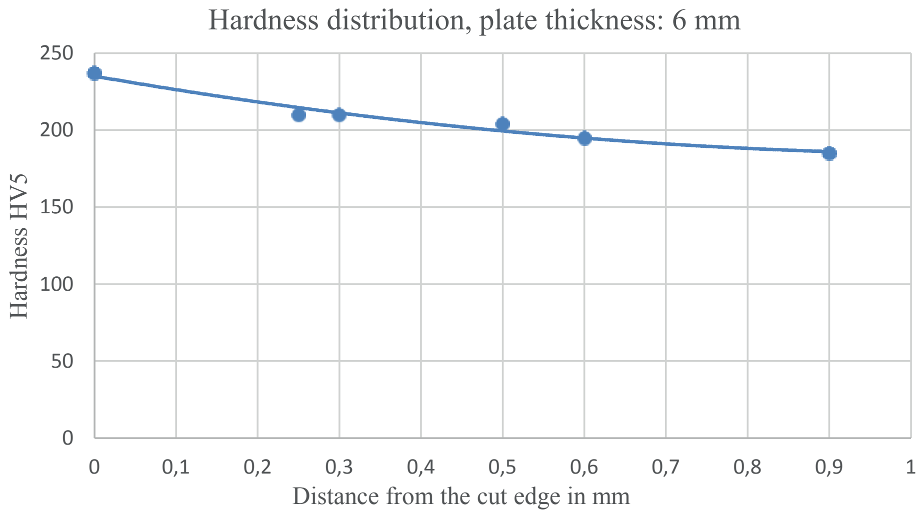

Fig. 14. Hardness distribution in the cross-section of the 6 mm thick specimen subjected to oxygen cutting

Summary

After oxygen cutting, the surface was characterised by significant smoothness, with few grooves and deviations of linearity. The surface also contained traces of cinder. The degradation of the profile was rather high, which resulted primarily from the heat source effect, responsible for the partial melting of the upper edge (frequently) and the formation of slag overhangs on the lower part. The width of the heat affected zone was also significant (approximately 1mm–1.5 mm), particularly in the upper area, on the side affected by the heat source. The HAZ tended to be wider in the thicker elements. The cut zone was also characterised by higher hardness – the higher, the thicker the material subjected to cutting. The maximum hardness values obtained in relation to the 20 mm and 12 mm thick plates exceeded the permissible values specified in requirements for welded joints. Because of the above-presented inconveniences, surfaces subjected to oxygen heating should be next subjected to treatment aimed to satisfy requirements related to welding processes. An undoubted advantage of oxygen cutting is its versatile applicability in non-mechanised, mechanised and automated processes. Oxygen cutting is also very useful within a wide range of structural materials in relation to fixing, refurbishment and repair works.

References

[1] Pałasz J.: Poradnik spawacza gazowego. Wydawnictwa Naukowo-Techniczne, Warszawa 1986.

[2] Czupryński A.: Podstawowe technologie spawalnicze w ćwiczeniach laboratoryjnych. Część pierwsza. Wydawnictwo Politechniki Śląskiej, Gliwice 2017.

[3] Klimpel A.: Spawanie, zgrzewanie i cięcie metali. Technologie. Wydawnictwa

Naukowo-Techniczne, Warszawa 2009.
[4] Ferenc K., Ferenc J.: Spawalnicze gazy osłonowe i palne. Wydawnictwa Naukowo-Techniczne, Warszawa 2013.
[5] Pilarczyk J. (edit.): Poradnik Inżyniera. Spawalnictwo, t. 2. Wydawnictwa Naukowo-Techniczne, Warszawa 2017.
[6] Ambroziak A. (edit.): Techniki wytwarzania. Spawalnictwo. Laboratorium. Oficyna Wydawnicza Politechniki Wrocławskiej, Wrocław 2010.
[7] Ferenc K.: Spawalnictwo. Wydawnictwa Naukowo-Techniczne, Warszawa 2005.
[8] Klimpel A., Mazur M.: Podręcznik spawalnictwa. Wydawnictwo Politechniki Śląskiej, Gliwice 2004.
[9] Pakos R.: Wpływ metody cięcia na właściwości stalowej krawędzi ciętej. Biuletyn Instytutu Spawalnictwa, 2012, no. 8, pp. 54–57.
[10] Słania J., Krawczyk R., Cieśla D.: Charakterystyka cięcia termicznego. Przegląd Spawalnictwa, 2015, vol. 87, no. 7, pp. 18–22.
[11] Krawczyk R., Słania J., Cieśla D.: Porównanie metod cięcia termicznego. Przegląd Spawalnictwa, 2015, vol. 87, no. 7, pp. 23–28.